Chapter 8

Gamma-Gamma Interaction

8.1 Gamma-Gamma Interaction Region

The scientific advantages of incorporating high-energy $\gamma\gamma$ collisions into an e^+e^- collider design have been discussed from the earliest collider physics meeting in Saariselka, Finland in 1989. $\gamma\gamma \rightarrow$ Higgs is a fundamental process that opens a window on new physics beyond the standard model. In the past, the technical challenges posed by the laser system and the interaction region seemed to be overwhelming and kept the option of a $\gamma\gamma$ collider out of the mainstream program. Recently, there has been sufficient progress on both these fronts to change that view and to allow the $\gamma\gamma$ collider to be considered a feasible addition to the LC project [1].

The required laser power is now available from the Mercury laser developed at LLNL for fusion applications. It is a relatively straightforward R&D effort to take the 100-joule, 10-Hz output of a Mercury laser and to shape its time structure to match that of the NLC running in $\gamma\gamma$ mode with 95 bunches separated by 2.8 ns. Only twelve such lasers would be required for both the electron and positron beams. Schemes being discussed as recently as 1995 called for hundreds of lasers costing billions of dollars; the current picture is technically and fiscally more viable.

The breakthrough in IR design has been the development of large annular optics which permit the laser beams to be focused to the required 10 micron spots without putting any material in the path of the residual electrons, noninteracting photons or charged particle debris arising from the beam-beam collision. These unwanted particles now can pass unimpeded down the extraction line. The performance of a fully engineered IR design based on such optics was simulated, and found to be adequate. While much work needs to be done in detailing the measures required to control the laser-beam quality in the IR environment, the fundamental problem has been resolved.

8.2 Laser Architecture

For maximum luminosity, every electron bunch should collide with a laser pulse of sufficient intensity that 63% of the electrons undergo a primary Compton backscatter. The laser pulse energy required to achieve this is minimized when the Raleigh range of the laser focus and the laser pulse width is matched to the 100-micron length of the electron bunch. However, to avoid nonlinear QED effects the maximum intensity must also be limited. A pulse of 1 joule in 1.8 ps FWHM optimizes the conversion. This corresponds to a peak power in the terawatt range. Such high peak power was made possible by the invention in 1985, of chirped pulse amplification [2,3].

For $\gamma\gamma$ operation, The NLC bunch structure consists of trains of 95 bunches separated by 2.8 ns, with 120 trains per second. This means that 11,400 laser pulses per second must be produced, requiring an average laser power of 10 kilowatts. Additionally, these pulses have to be produced with the correct temporal spacing to match the electron-bunch structure. No current laser architecture can achieve all of these requirements at once. However, the Mercury laser, developed for a laser-fusion application, can be modified to deliver the required pulse format. The Mercury laser, as shown in Fig. 8.1, has two amplifier heads, allowing four amplification passes. Running at 10 Hz it can produce pulses of 100 joules with a pulse width of a couple of nanoseconds. The single pulse of 100 joules can be subdivided into 100 1-joule pulses separated by 2.8 ns either through modification of the front end or through a combination beam splitter and optical delay line. A set of twelve of these lasers, each running at 10 Hz, could then be combined to provide the 120 Hz required for the NLC.

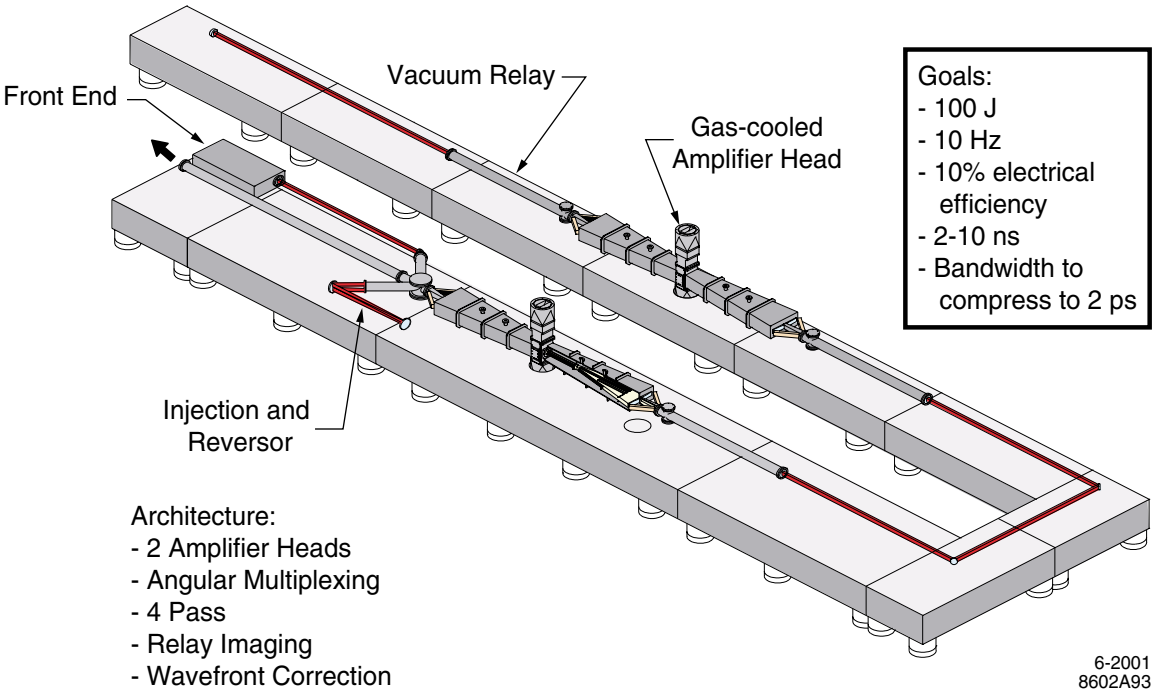

Figure 8.1: The diode-pumped solid state Mercury laser is a high pulse rate, next-generation laser fusion driver.

The Mercury laser combines several key technologies (see Fig. 8.2) to achieve the required performance. The Ytterbium-Strontium-Fluorappetite Yb:S-FAP crystals are pumped by diode arrays. Since the diode output can be tuned to the pump band of the crystals, they can achieve an efficiency of 10% for converting wall plug power to laser light. The long upper-state lifetime of the crystals allows the laser to be pumped more slowly, reducing the required peak diode power. This is a great advantage since the diode arrays are the cost driver for the system. The waste heat deposited in the crystal is removed by helium gas flowing perpendicular to the crystal plates. This minimizes thermal distortion and allows the laser to produce high average power while retaining good beam quality.

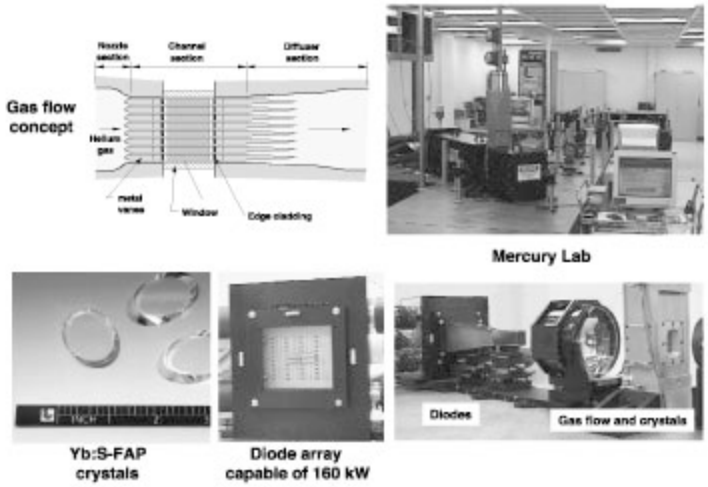

Figure 8.2: The Mercury laser will utilize three key technologies: gas cooling; diodes; and Yb:S-FAP crystals to deliver 100 J at 10 Hz with 10% efficiency.

8.3 Optics and Interaction Region

The laser pulse and the electron bunch intersect 5-mm away from the interaction point. The optics required to focus the laser must be located in the confined space of the interaction point (IP). They must be situated such that they do not interfere with the accelerator or degrade the performance of the detector. Figure 8.3 shows a schematic of the interaction region with the beam pipe, masks, detector components and optics, starting from the standard design of the e^+e^- interaction region. The intensity of the laser beams requires that they be propagated in vacuum and that transmissive optics be kept to a minimum. Therefore, the optics are located in the beam pipe which is enlarged to accommodate them. The three small mirrors provide the ability to adjust the focus while the large final optic allows the beam to be focused to a 10-micron diameter spot. Not shown in Fig. 8.3 is a complementary set of mirrors on the other side of the IP. They catch the laser pulse, reflect it and refocus it onto the opposite electron beam. Thus each laser pulse does double duty and reduces the total required laser power.

To prevent the material of the mirrors from contributing to detector backgrounds they have been placed such that they avoid the incoming and outgoing beams and the pair background. The smaller mirrors pose no problem but the large mirror requires a large hole in the center to prevent the pair background from showering in it. This requires the laser pulse to be preshaped to be cylindrical.

One other modification to the interaction region is required. The extraction-line aperture must be increased to +/– 10 milliradians to accommodate the increased outgoing beam divergence in $\gamma\gamma$ collisions. To prevent interference between the extraction line and the final- focus quadropole, the crossing angle is increased from 20 to 30 milliradians. Once a detailed design of the final-focus quadrupole is available this angle should be made as small as possible. The increased extraction-line aperture has an effect on the detector. The first two layers of the SVX now have a direct line of sight back to the beam dump and will

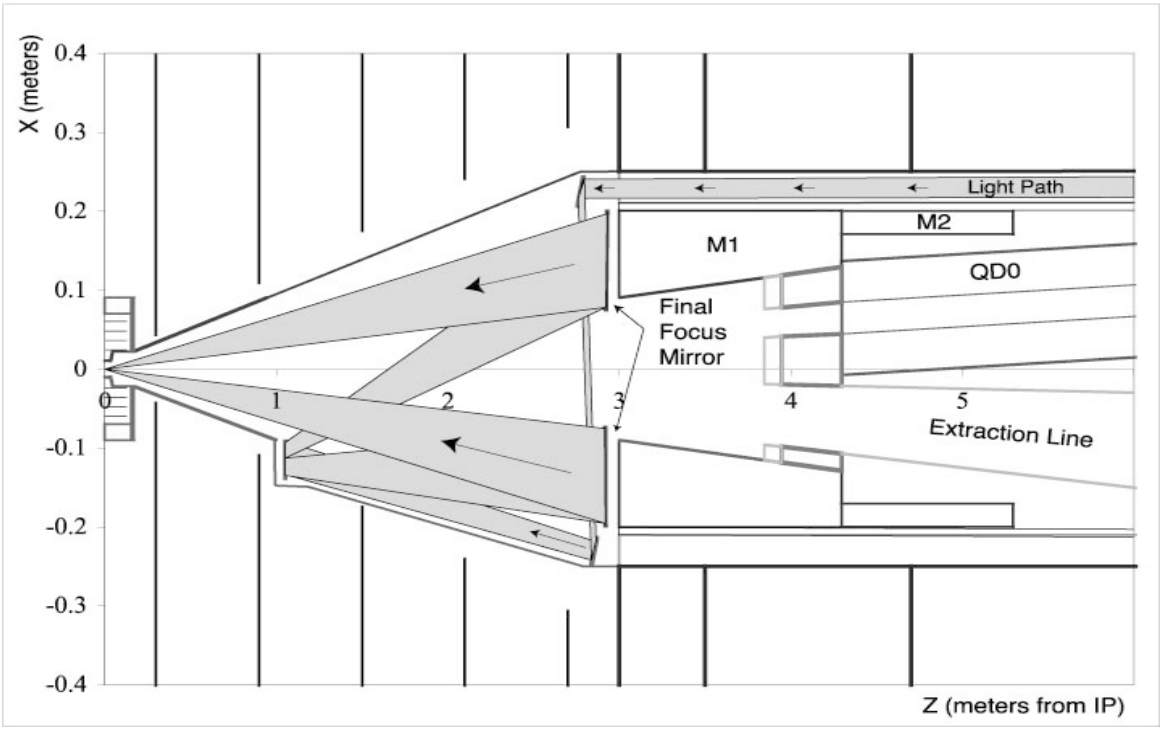

Figure 8.3: Optical configuration to inject the laser light into the Interaction Region. The high subpulse intensity requires all these optics to be reflective and mounted inside the vacuum enclosure.

see a flux of 10^{11} neutrons/cm^2/year. The standard CCDs will need to be replaced with a more radiation-hard technology.

8.4 The Benchmark $\gamma\gamma \rightarrow H \rightarrow b\bar{b}$ mode

The measurement of the two-photon width of the Higgs is one of the main physics analyses for a photon collider. Since $\gamma\gamma \rightarrow$ H proceeds through a loop diagram and all particles with mass and charge can contribute to it, this mode is an excellent probe of new physics beyond the standard model. For this design of the laser and optics, the CAIN [4] program has been used to simulate the $\gamma\gamma$ luminosity spectrum. Figure 8.4 shows the calculated luminosity for running conditions optimized for a 120-GeV Higgs. The high-energy peak is dominated by photons from primary Compton backscatters. The low-energy tail comes from photons produced when spent electrons multiply interact with the laser and from beamstrahlung photons. Using 80% electron polarization and 100% circular polarization of the laser enhances the peak luminosity and allows control of the spin state. This allows an enhancement of the spin 0 $\gamma\gamma \rightarrow$ H mode and suppression of the standard model background $\gamma\gamma \rightarrow b\bar{b}$ which proceeds through spin 2 [5].

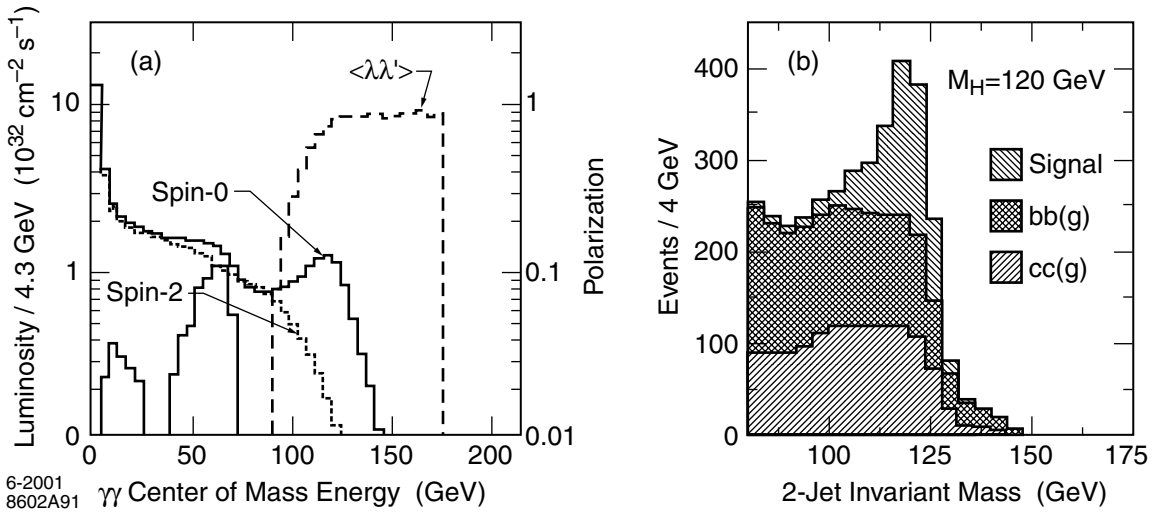

Figure 8.4: $\gamma\gamma$ luminosity distribution for Higgs factory running is shown in plot (a) as luminosity per 4.3-GeV bin and the Higgs to $b\bar{b}$ signal and backgrounds are shown in (b) as events per 4 GeV bin after integrating 10^7 s.

References

[1] American Linear Collider Working Group, *Linear Collider Physics Resource Book for Snowmass 2001*, BNL-52627, CLNS 01/1729, Fermilab-Pub-01/058-E, LBNL-47813, SLAC-R-570, UCRL-ID-143810-DR, LC-REV-2001-074-US.

[2] Strickland, D. and Mourou G., "Compression of amplified chirped optical pulses," *Opt. Commun.* **56**:219-221, 1985.

[3] Perry, M.D. and Mourou G., "Terawatt to petawatt sub-picosecond lasers," *Science*, **264**:917-924, 1994.

[4] Yokoya, K., "A Computer Simulation Code for the Beam-Beam Interaction in Linear Colliders", KEK Report 85-9, October 1985.

[5] Asner, D., Gronberg, J., Gunion, J. and Hill T., UCRL-ID-143967.